



# EXPERIMENTAL RESULTS OF AN ACTIVE SIDEWALL PANEL WITH VIRTUAL MICROPHONES FOR AIRCRAFT INTERIOR NOISE REDUCTION

Malte Misol
*German Aerospace Center (DLR), Institute of Composite Structures and Adaptive Systems, Germany*
*e-mail: malte.misol@dlr.de*
Stephan Algermissen
*German Aerospace Center (DLR), Institute of Composite Structures and Adaptive Systems, Germany*
*email: stephan.algermissen@dlr.de*

This work focuses on the reduction of aircraft interior noise by means of actively controlled sidewall panels (smart linings). It was shown in prior work that considerable reductions of interior sound pressure level can be achieved using structural actuators on the lining and microphones distributed in the seat area in front of the linings. Simulation results suggest that the physical microphones in front of the linings can be replaced by so-called virtual microphones. The signals of these virtual microphones are obtained from filtering the normal surface vibrations of the lining through an observer filter. Accelerometers are mounted on the lining structure to obtain the vibration signals. Simulation results of a smart lining with virtual microphones show a mean sound pressure level (SPL) reduction of 10 dB and 5.9 dB(A) in front of the lining. These results must be verified by laboratory experiments applying real-time control because the effects of time variances and imperfect path models will deteriorate the performance of the smart lining. Therefore, the present contribution describes an experimental realization of a smart lining with remote sensors and virtual microphones in a realistic laboratory setup. A double panel system consisting of a primary carbon fiber reinforced plastic (CFRP) structure (fuselage) and a coupled smart lining is installed in the opening of a transmission loss facility. The real-time behavior of the smart lining is tested and the influence of using virtual instead of physical microphones on the SPL reduction is quantified. One focus is on evaluating the robustness of the smart lining under changing environmental conditions.

Keywords: aircraft, interior noise, active control, remote sensors, virtual microphones

## 1. Introduction

Active noise control is able to reduce cabin noise in propeller driven aircraft. Different approaches are pursued since the late 1980s. One approach followed by Elliott et al. [1] uses loudspeakers to generate

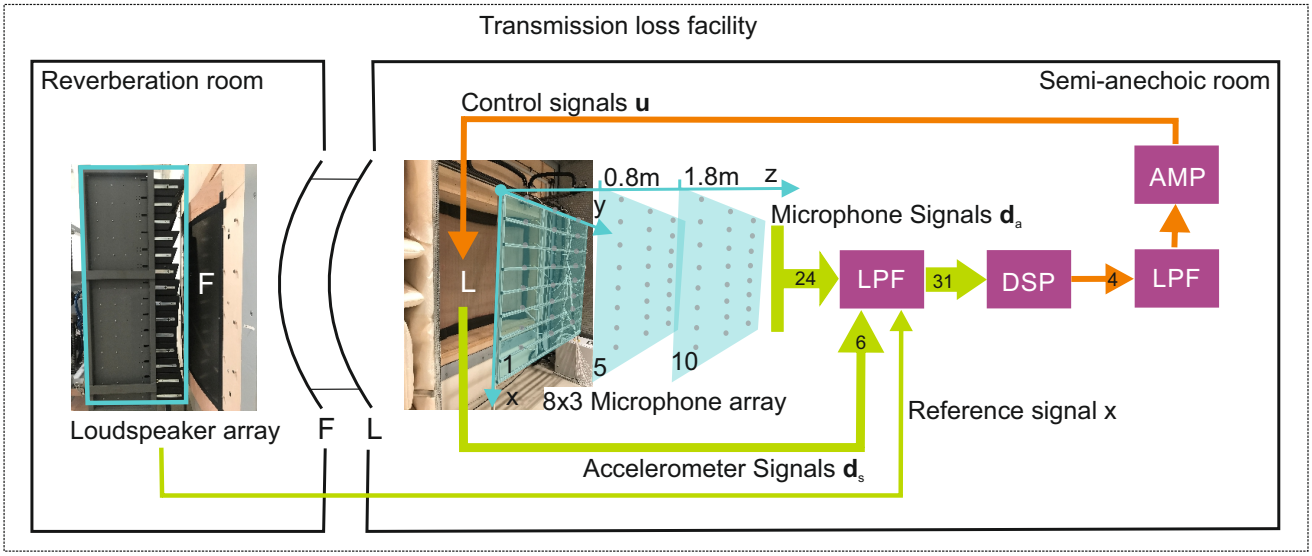


Figure 1: Experimental setup in the sound transmission loss facility.

anti-sound which destructively interferes with the cabin noise. An alternative approach is the active structural acoustic control (ASAC). The ASAC method requires structural actuators and sensors to control the sound radiating structural vibration of surfaces. Early results of ASAC are published by Fuller and Jones [2]. One realization of an ASAC system uses actuators and sensors applied to the sidewall panels (linings). Early experiments with such active linings are documented in Lyle and Silcox [3]. Active linings with electrodynamic exciters as actuators are successfully realized by Misol et al. [4] and by Misol [5]. In [4] tests of an active lining in a sound transmission loss facility and in [5], full-scale tests of two active lining modules mounted in the cabin of a Dornier Do728 aircraft are reported.

The active noise control systems mentioned so far have in common that they use microphones as error sensors. However, the requirement of having distributed and closely adjacent microphones in the whole cabin is undesirable because it requires additional wiring and prevents flexible cabin layouts. The so-called smart lining concept proposed by Misol et al. [4] tries to overcome these drawbacks by modular active linings with structurally integrated actuators, sensors and control. This concept requires a substitution of the physical error microphones by virtual error microphones. One applicable method is the remote microphone technique for active control proposed by Roure and Albarazzin [6]. In this technique the error microphones are substituted by remote microphones and an observer filter. In a similar approach, Cheer and Daley [7] replace the remote microphones by accelerometers mounted on the radiating structure. This approach is adopted for the smart lining concept. However, as will be discussed later in this paper, this choice of remote structural sensors introduces a feedback path into the control plant which is sensitive to changes in the environmental conditions. In order to quantify this sensitivity in terms of control performance, the present contribution focuses on the performance and robustness of the active lining panel in the case of imperfect secondary path models. The analysis is based on measurement data and identified frequency response function (FRF) models of an aircraft typical laboratory setup.

## 2. Experiments

The experiments are done in the sound transmission loss facility of the German Aerospace Center (DLR). The experimental setup is shown in Fig. 1. The smart lining panel (L) is attached to the fuselage structure (F) which itself is mounted in the test opening of the facility. The fuselage is acoustically excited

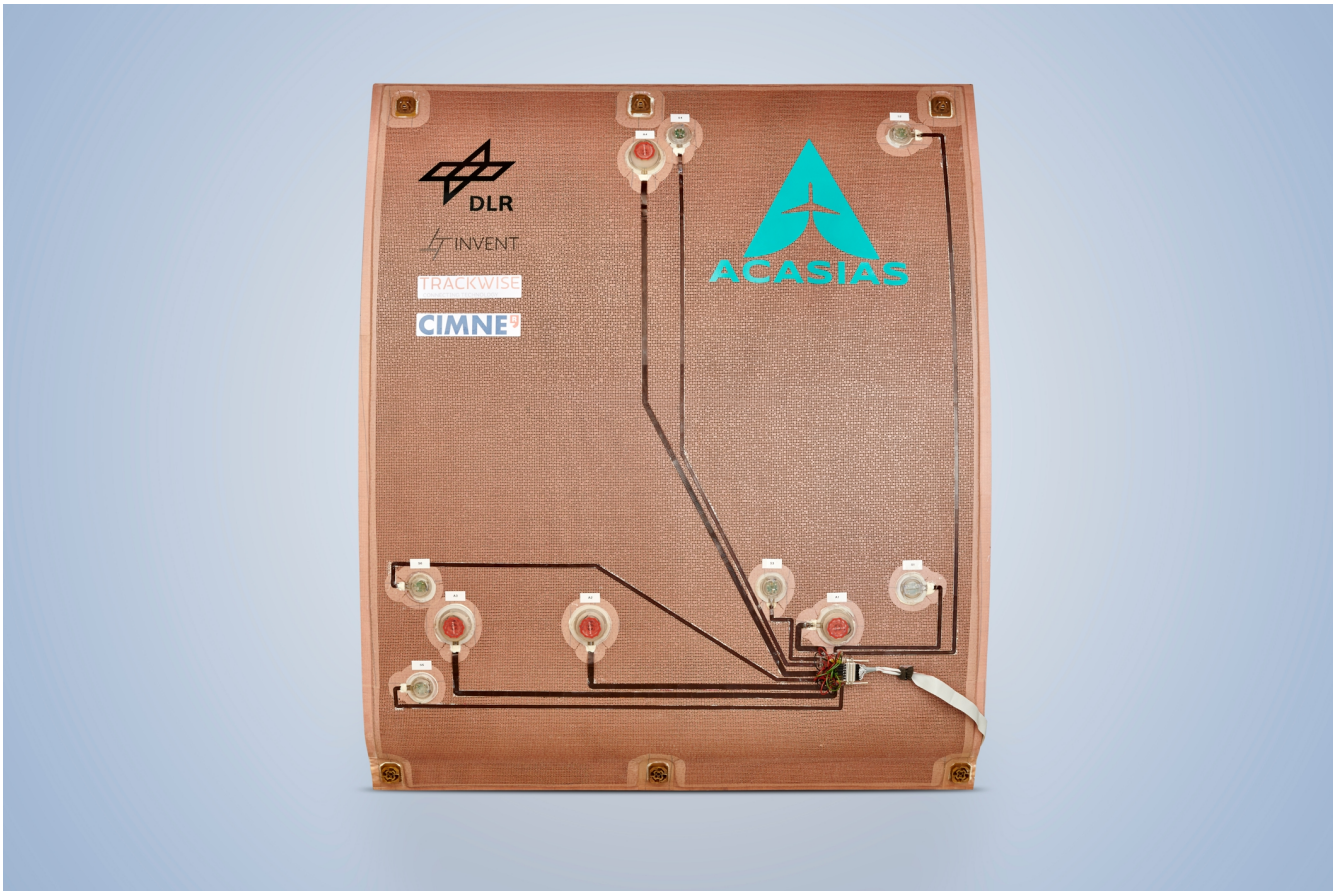


Figure 2: Backside of the smart lining panel equipped with four inertial exciters (red) and six accelerometers (green).

from the reverberation room by means of a loudspeaker array. The excitation sound field is typical for a counter rotating open rotor (CROR) engine. It contains the first five harmonics at 119.4 Hz, 149.2 Hz, 268.6 Hz, 387.5 Hz and 417.9 Hz. The transmitted sound is measured in the semi-anechoic room by means of a microphone array with 24 microphones. Measurements are repeated for ten different distances between microphone plane and lining. The reference signal $x$ originating from the analog output of the loudspeaker array is used to assemble the signals from the sequential measurements correctly. The hardware used for data sampling and real-time control is a MicroLabBox from dSPACE (DSP). The sampling rate is set to 2000 Hz. All analog input and output signals are bandlimited to 500 Hz using low-pass filters (LPF). The control signals are amplified with a power amplifier (AMP). The signals from the accelerometers $\mathbf{d_s}$, microphones $\mathbf{d_a}$ and the reference signal $x$ are used as inputs for the control plant shown in Fig. 3.

The smart lining panel is equipped with four inertial exciters (actuators) and six accelerometers (sensors). The actuator and sensor locations and the wiring is shown in Fig. 2. The actuators and sensors are mounted to the sandwich panel structure by means of inserts. These inserts facilitate an easy mounting and dismounting of the transducers via a bayonet connector with integrated spring contacts for the electrical signals. Furthermore, the inserts protect the transducers from dust and humidity. The wiring is realized by ultra thin and lightweight isolated ribbon cables which all meet in a common connector point.

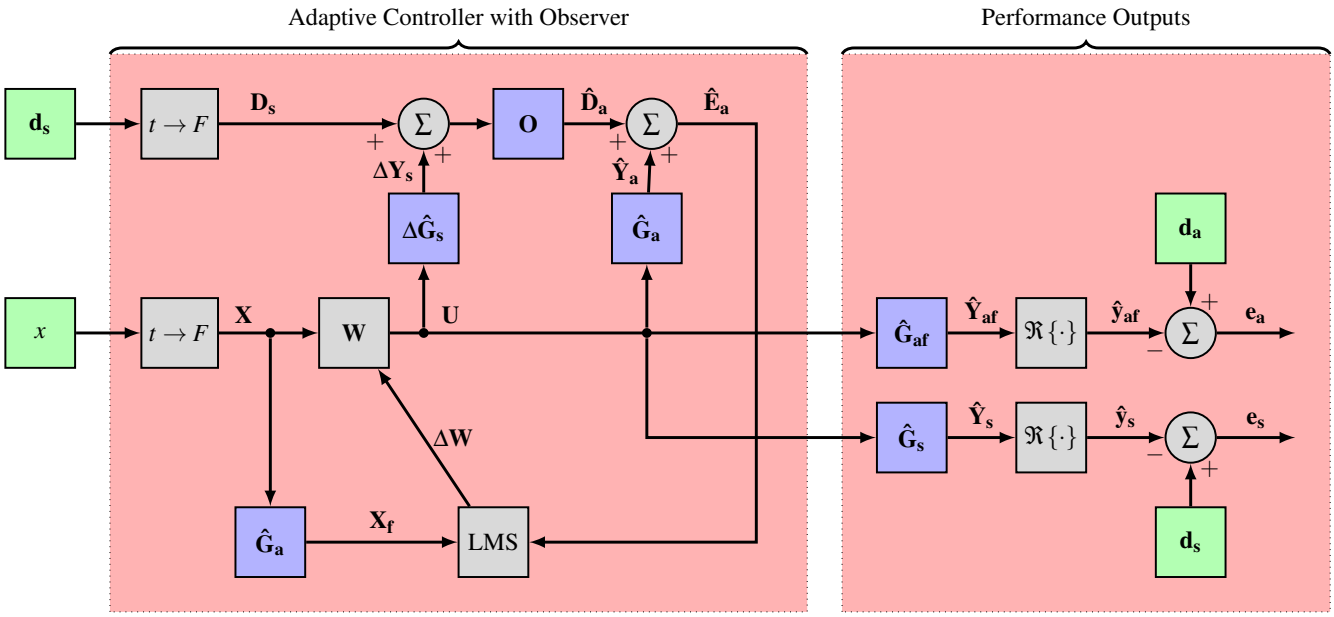


Figure 3: Block diagram of the control plant.

## 3. Simulations

A block diagram of the control plant is shown in Figure 3. The green blocks are input signals and the blue blocks are FRF models both obtained from experiments. The grey blocks perform linear operations on the signals. A detailed description of the control plant and its blocks can be found in Misol [9]. The observer filter $\mathbf{O}$ is defined in [9, Eq. 2] and the adaptation law for the control filter weights is given in [9, Eq. 5)]. However, in [9] the actuator feedback on the remote sensors is assumed to be fully compensated by a perfect structural secondary path model $\hat{\mathbf{G}}_\mathbf{s}$. The present contribution rejects this assumption and investigates the robustness and the noise reduction performance of the active lining in the case of an imperfect structural secondary path model. The deviations of the secondary path model from the real physical plant are attributed to changing environmental conditions. To account for these deviations a block $\Delta\hat{\mathbf{G}}_\mathbf{s}$ is introduced into the control plant. The simulation model of the control plant with this additional block permits a numerical estimation of the real-time control in the case of imperfect structural secondary path model. If $\Delta\hat{\mathbf{G}}_\mathbf{s} \neq 0$ the actuator feedback leads to a distortion of the remote sensor signals $\mathbf{D_s}$ by the control signals $\mathbf{U}$. It can be seen in Fig. 4 that the structural secondary path $\mathbf{G_s}$ is temperature dependent. Hence, if $\hat{\mathbf{G}}_\mathbf{s}$ is identified at temperature $T_1$ and the real-time control is performed at temperature $T_2$, it must be analyzed how the temperature induced inaccuracy of the structural secondary path model affects the control performance.

Equation 1 reveals how the estimated acoustic error signal $\hat{\mathbf{E}}_\mathbf{a}$ is influenced by uncompensated actuator feedback.

$$\hat{\mathbf{E}}_\mathbf{a} = \mathbf{O}\mathbf{D_s} + \overbrace{(\hat{\mathbf{G}}_\mathbf{a} + \mathbf{O}\Delta\hat{\mathbf{G}}_\mathbf{s})}^{\tilde{\mathbf{G}}_\mathbf{a}}\mathbf{U} \tag{1}$$

It is assumed that the structural secondary path is identified at temperature $T_2$ but real-time control is performed at $T_1$. In this case $\Delta\hat{\mathbf{G}}_\mathbf{s} = \hat{\mathbf{G}}_\mathbf{s}^{T_1} - \hat{\mathbf{G}}_\mathbf{s}^{T_2}$ describes the difference between the structural secondary path models at temperatures $T_1$ and $T_2$. It is further assumed that the acoustic secondary path $\mathbf{G_a}$ is constant over temperature and is accurately modelled by the acoustic secondary path model $\hat{\mathbf{G}}_\mathbf{a}$. If

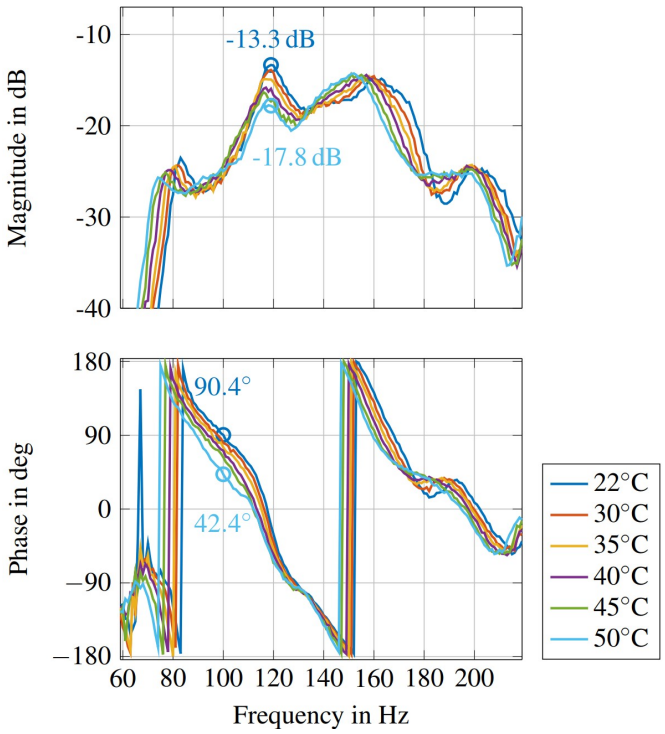


Figure 4: Bode plot of structural secondary path $\mathbf{G_s}$ in dependence of the temperature [8].

$T_1 \neq T_2 \rightarrow \Delta\hat{\mathbf{G}}_\mathbf{s} \neq 0$ and the effective acoustic secondary path is $\tilde{\mathbf{G}}_\mathbf{a} = \hat{\mathbf{G}}_\mathbf{a} + \mathbf{O}\Delta\hat{\mathbf{G}}_\mathbf{s}$. According to Elliott [10, p. 201], the adaptive controller is only stable if all eigenvalues $\lambda$ of the matrix $[\hat{\mathbf{G}}_\mathbf{a}{}^H\tilde{\mathbf{G}}_\mathbf{a} + \beta I]$ are positive. $I$ is the identity matrix of proper dimension. A nonzero effort weighting factor $\beta$ can be used to stabilize the system. The gained robustness by a nonzero $\beta$ is however at the expense of a reduced noise reduction performance. It will be shown in the following Section that a nonzero $\beta$ is required to stabilize certain harmonics if temperature variations occur.

## 4. Results

Figure 5 shows the sound pressure level (SPL) distribution on the microphone planes 1, 5 and 10 (see Fig. 1) for the uncontrolled case (a) and for three different temperature scenarios (b), (c) and (d). The other microphone planes are omitted for reasons of clarity. This is possible because the SPL distribution between the planes 1, 5, and 10 is continuous and smooth. The locations of the virtual microphones are indicated by red dots. The underlying data of Fig. 5 is from the performance output $\mathbf{e_a}$ in Fig. 3. The sound pressure reductions are calculated relative to the measured disturbance sound pressures $\mathbf{d_a}$. In the uncontrolled case (a), a decrease of the sound pressure level can be seen with increasing distance ($z$) from the lining. Scenario (b) represents the ideal control scenario with $\Delta\hat{\mathbf{G}}_\mathbf{s} = 0$. This means either constant temperature conditions or perfect (temperature dependent) secondary path modeling. In this scenario a mean SPL reduction of 10 dB and 5.9 dB(A) is achieved on plane 1 ($z = 0$) and a mean SPL reduction of 8 dB and 5.7 dB(A) is achieved on planes 1–10 (240 virtual microphones). In scenario (c) it is assumed that the structural secondary path model $\hat{\mathbf{G}}_\mathbf{s}{}^{T_2}$ is identified for $T_2 = 30$°C and the temperature during real-time control is $T_1 = 22$°C (or vice versa). This means $\Delta\hat{\mathbf{G}}_\mathbf{s} \neq 0$ corresponding to an imperfect compensation of the actuator feedback on the remote sensors (accelerometers). In this scenario all eigenvalues $\lambda$ are positive, but the smallest eigenvalue associated with the frequency of the

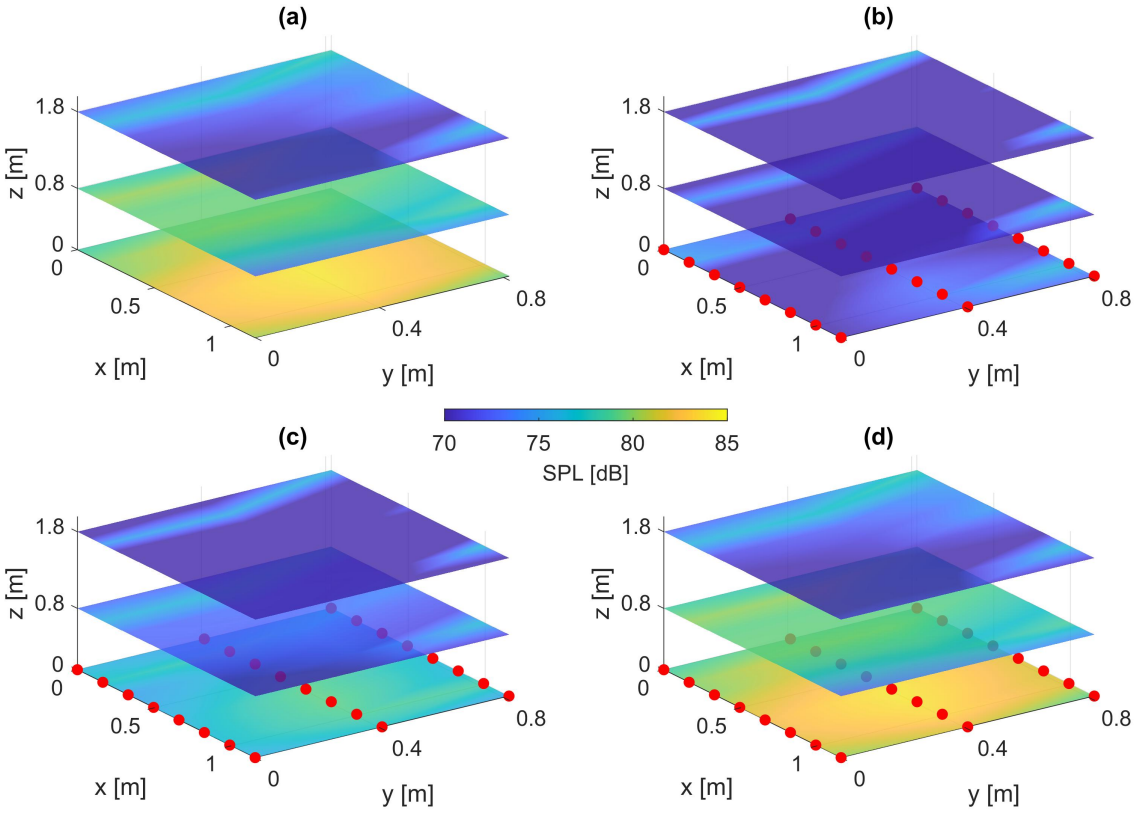


Figure 5: SPL distribution on three planes in front of the lining for the uncontrolled case (a) and for three different temperature scenarios (b)–(d).

second harmonic is close to zero and must be stabilized by taking $\beta = 0.0366$. The implications on control performance are visible in Fig. 5 (c). A mean SPL reduction of 4.5 dB and 3.2 dB(A) is achieved on plane 1 ($z = 0$) and a mean SPL reduction of 4.8 dB and 3.9 dB(A) is achieved on planes 1–10. A further degradation of control performance occurs in scenario (d) where it is assumed that the structural secondary path model $\hat{\mathbf{G}}_{\mathbf{s}}^{T_2}$ is identified for $T_2 = 35°\text{C}$ and the temperature during real-time control is $T_1 = 22°\text{C}$ (or vice versa). In this scenario the smallest eigenvalues associated with the frequencies of the first and the second harmonic are negative and must be stabilized by taking $\beta = 3.2764$ for the first and $\beta = 2.0947$ for the second harmonic. Such strong control weighting implies that the SPL at the first two harmonics will not be affected by the active controller. Since these two harmonics dominate the SPL, Fig. 5 (a) and (d) are very similar. In scenario (d) a mean SPL reduction of 0.14 dB and 0.13 dB(A) is achieved on plane 1 ($z = 0$) and a mean SPL reduction of 0.11 dB and 0.013 dB(A) is achieved on planes 1–10. The results clearly underline that a temperature compensation of the secondary path model is useful and might be necessary. However, it is unclear how much the temperature of the lining actually varies during flight since, as an interior part, it is thermally coupled to the cabin and isolated from the fuselage by an air gap filled with glass fiber insulation bags. Furthermore, the variation of the acoustic secondary path $\mathbf{G}_{\mathbf{a}}$ due to changes in temperature, seat occupation and other factors will have a negative influence on the noise reduction performance as well. But it will not affect the stability of the control system since the acoustic secondary path model $\hat{\mathbf{G}}_{\mathbf{a}}$ is an integral part of the adaptive controller with virtual microphones (see Fig. 3). It remains a future task to assess the implications of imperfect acoustic

secondary path models on the control performance.

## 5. ACKNOWLEDGEMENTS

This project has received funding from the European Union's Horizon 2020 research and innovation programme under grant agreement No. 723167.

## REFERENCES

1. Elliott, S. J., Nelson, P. A., Stothers, I. M. and Boucher, C. C. In-flight experiments on the active control of propeller-induced cabin noise, *Journal of Sound and Vibration*, **140** (2), 219–238, (1990).

2. Fuller, C. R. and Jones, J. D. Experiments on reduction of propeller induced interior noise by active control of cylinder vibration, *Journal of Sound and Vibration*, **112** (2), 389–395, (1987).

3. Lyle, K. H. and Silcox, R. J. A study of active trim panels for interior noise reduction in an aircraft fuselage, *SAE Technical Paper*, 05, SAE International, (1995).

4. Misol, M., Algermissen, S., Rose, M. and Monner, H. P. Aircraft lining panels with low-cost hardware for active noise reduction, *Joint Conference ACOUSTICS 2018*, (2018).

5. Misol, M. Full-scale experiments on the reduction of propeller-induced aircraft interior noise with active trim panels, *Applied Acoustics*, **159**, 107086, (2020).

6. Roure, A. and Albarrazin, A. The remote microphone technique for active noise control, *PROCEEDINGS OF ACTIVE 99: THE INTERNATIONAL SYMPOSIUM ON ACTIVE CONTROL OF SOUND AND VIBRATION, VOLS 1 & 2*, pp. 1233–1244, (1999).

7. Cheer, J. and Daley, S. Active structural acoustic control using the remote sensor method, *Journal of Physics: Conference Series*, **744** (1), (2016).

8. Algermissen, S. and Misol, M. Experimental Analysis of the ACASIAS Active Lining Panel, Martinez, X. and Schippers, H. (Eds.), *Proc. of European Conference on Multifunctional Structures (EMuS)*, online event, November 17–18, (2020).

9. Misol, M. Active Sidewall Panels with Virtual Microphones for Aircraft Interior Noise Reduction, *Applied Sciences*, **10** (6828), 1–13, (2020).

10. Elliott, S. J., *Signal Processing for Active Control*, Academic Press, London (2001).